INTERNATIONAL JOURNAL OF Experimental Pathology

Int. J. Exp. Path. (2015), 96, 42–53

ORIGINAL ARTICLE

Exogenous connexin43-expressing autologous skeletal myoblasts ameliorate mechanical function and electrical activity of the rabbit heart after experimental infarction

Ieva Antanavičiūtė*, Eglė Ereminienė†, Vaidas Vysockas*,‡, Mindaugas Račkauskas*,‡, Vilius Skipskis§, Kristina Rysevaitė¶, Rimantas Treinys*, Rimantas Benetis*,‡, Jonas Jurevičius* and Vytenis A. Skeberdis*

**Institute of Cardiology, Medical Academy, Lithuanian University of Health Sciences, Kaunas, Lithuania, †Department of Cardiology, Medical Academy, Lithuanian University of Health Sciences, Kaunas, Lithuania, ‡Department of Cardiac, Thoracic and Vascular Surgery, Medical Academy, Lithuanian University of Health Sciences, Kaunas, Lithuania, §Department of Non-infectious Diseases, Veterinary Academy, Lithuanian University of Health Sciences, Kaunas, Lithuania and ¶Institute of Anatomy, Medical Academy, Lithuanian University of Health Sciences, Kaunas, Lithuania*

INTERNATIONAL JOURNAL OF EXPERIMENTAL PATHOLOGY

doi: 10.1111/iep.12109

Received for publication: 5 June 2014
Accepted for publication: 26 October 2014

Correspondence:
Vytenis A. Skeberdis
Institute of Cardiology
Lithuanian University of Health Sciences
Sukilėlių pr. 17
50009 Kaunas
Lithuania
Tel.: +370 37 302880
Fax: +370 37 302872
E-mail: arvydas.skeberdis@lsmuni.lt

SUMMARY

Acute myocardial infarction is one of the major causes of mortality worldwide. For regeneration of the rabbit heart after experimentally induced infarction we used autologous skeletal myoblasts (SMs) due to their high proliferative potential, resistance to ischaemia and absence of immunological and ethical concerns. The cells were characterized with muscle-specific and myogenic markers. Cell transplantation was performed by injection of cell suspension (0.5 ml) containing approximately 6 million myoblasts into the infarction zone. The animals were divided into four groups: (i) no injection; (ii) sham injected; (iii) injected with wild-type SMs; and (iv) injected with SMs expressing connexin43 fused with green fluorescent protein (Cx43EGFP). Left ventricular ejection fraction (LVEF) was evaluated by 2D echocardiography *in vivo* before infarction, when myocardium has stabilized after infarction, and 3 months after infarction. Electrical activity in the healthy and infarction zones of the heart was examined *ex vivo* in Langendorff-perfused hearts by optical mapping using di-4-ANEPPS, a potential sensitive fluorescent dye. We demonstrate that SMs in the coculture can couple electrically not only to abutted but also to remote acutely isolated allogenic cardiac myocytes through membranous tunnelling tubes. The beneficial effect of cellular therapy on LVEF and electrical activity was observed in the group of animals injected with Cx43EGFP-expressing SMs. L-type Ca^{2+} current amplitude was approximately fivefold smaller in the isolated SMs compared to healthy myocytes suggesting that limited recovery of LVEF may be related to inadequate expression or function of L-type Ca^{2+} channels in transplanted differentiating SMs.

Keywords
2D echocardiography, autologous skeletal myoblast transplantation, connexin43, intercellular communication, myocardial infarction, optical mapping

Ischaemic heart disease and myocardial infarction (MI) lead among the major causes of mortality worldwide. Heart failure following MI results from acute loss of myocytes in the infarction zone and pathologic remodelling of the ventricle. In animal models, the experimental MI causes death of 5–30% of the myocytes in the heart (Mani & Kitsis 2003). As natural mechanisms of heart self-renewal have a low potential, the replacement of lost cardiomyocytes (CMs) is the main goal of heart regeneration. Among many other types of stem cells considered for regeneration of the heart

© 2014 The Authors.

(reviewed in Henning 2011; Shah and Shalia 2011; Hassan *et al.* 2014), autologous skeletal myoblasts (SMs) are acceptable candidates due to their high proliferative potential, resistance to ischaemia, easy isolation from muscle biopsy, and absence of tumorigenicity, immunological and ethical concerns. Animal studies have shown a positive effect of autologous SM transplantation on heart function (Durrani *et al.* 2010; Kolanowski *et al.* 2014), but the data obtained from phase I clinical trials, which failed to demonstrate functionally effective heart regeneration after infarction, are controversial (Menasche *et al.* 2008; Seidel *et al.* 2009; Brickwedel *et al.* 2014). The efficiency of SMs can be improved using cells overexpressing prosurvival genes (such as Akt) or angiogenesis-initiating genes (such as vascular endothelial growth factor) (Mangi *et al.* 2003; Haider *et al.* 2004) or preconditioning SMs with growth factors (Kofidis *et al.* 2004; Kanemitsu *et al.* 2006; Haider *et al.* 2008; Haider & Ashraf 2009). As donor cell death in the cardiac muscle is mainly caused by oxidative stress and inflammation, heat treatment has also been shown to contribute to the improvement of the efficiency of stem cell therapy (Suzuki *et al.* 2000; Nakamura *et al.* 2006; Kojima *et al.* 2007; Yang *et al.* 2007). Our recent study has demonstrated that in SMs, hyperthermia may stimulate the expression of total Cx43 protein and improve gap junction (GJ) function (Antanaviciute *et al.* 2014a).

The main disadvantage of SM application is an increased risk of ventricular tachyarrhythmias (Fernandes *et al.* 2006; Sherman *et al.* 2009). The pathogenesis of these arrhythmias is poorly understood. One of the reasons may be downregulation of endogenous GJ protein connexin43 (Cx43) during SM differentiation (Balogh *et al.* 1993; Reinecke *et al.* 2000; Menasche 2009). It has been shown by other authors that transplanted SMs cannot transdifferentiate into CMs and are committed to form the skeletal muscle in the heart (Murry *et al.* 1996; Reinecke *et al.* 2002). Implanted SMs proliferate up to 3 days and then differentiate to form multinucleated myotubes without electromechanical coupling between host CMs because the expression of two key proteins, N-cadherin and connexin, which are involved in electromechanical cell integration, is downregulated *in vivo* (Reinecke *et al.* 2000; Leobon *et al.* 2003). Cx43 is the most abundant GJ protein in the ventricular myocardium responsible for electrical and metabolic communication between CMs. Therefore, the overexpression of Cx43 could be a useful strategy to improve the therapeutic benefit of SMs. For example, enhanced GJ formation between SMs and CMs and decreased arrhythmogenicity were observed when SMs overexpressing Cx43 were transplanted into the heart (Abraham *et al.* 2005; Roell *et al.* 2007; Kolanowski *et al.* 2014). However, in the study by Fernandes *et al.* (2009) improved electrical coupling after implantation of SMs expressing exogenous Cx43 was not sufficient to prevent ventricular arrhythmias. The benefit is associated with efficient electrical incorporation of engrafted cells into the infarcted myocardium where the majority of myocytes are lost. It is not clear how transplanted cells synchronize with remote host myocytes under such acute conditions. Moreover, there are no data on how the transplantation of Cx43-transfected SMs affects mechanical function and electrical activity of the ventricles after MI.

In this study, we used the acute MI model to examine the effect of endocardial transplantation of autologous SMs transfected with Cx43EGFP on electromechanical function of the rabbit heart and discussed advantages and limitations of this approach. The novelty of our results is following: (i) our study is the first demonstrating the effect of Cx43-transfected SM transplantation on the recovery of left ventricular ejection fraction (LVEF) after infarction by 2D echocardiography; (ii) we used the potential sensitive optical dye di-4-ANEPS to demonstrate the impact of SM transplantation on the recovery of electrical activity in infarcted ventricles; (iii) we confirmed that SMs can form GJs with abutted CMs and demonstrate for the first time that SMs can couple electrically to the remote myocytes through membranous tunnelling tubes (TTs); and (iv) our results suggest that the limited recovery of LVEF may be related to inadequate expression or function of L-type Ca^{2+} channels in transplanted differentiating SMs.

Materials and methods

Isolation and culturing of SMs

Autologous SMs were isolated one month before MI induction. A piece of the femoral skeletal muscle (0.5 cm^3) of a New Zealand white rabbit was taken under general anaesthesia and placed into the transportation medium [Iscove's modified Dulbecco's medium (IMDM) with antibiotics, penicillin 300 U/ml and streptomycin 300 μg/ml]. The tissue was mechanically cut into smaller pieces and treated with an enzyme mixture: 1 mg/ml collagenase type V, 0.3 mg/ml hyaluronidase IV-S, 0.125% trypsin and 0.1% EDTA in PBS. After washing with IMDM, the cells were seeded in flasks with a culture medium (IMDM, 10% FBS, penicillin 100 U/ml and streptomycin 100 μg/ml).

Ethical Approval

Our investigation conforms to the European Community guidelines for the care and use of animals (86/609/CEE, CE Off J no. L358, 18 December 1986). The licence for the use of laboratory animals (No. 0171, 31 October 2007) was received from the Lithuanian Food and Veterinary Service.

Immunocytochemistry

The cells grown on glass coverslips were fixed with 4% paraformaldehyde for 15 min. Then, the cells were washed with PBS and incubated in PBS with 0.2% Triton X-100 for 3 min to permeabilize membranes. After blocking in PBS with 1% BSA for 1 h, the coverslips were incubated with primary antibodies against desmin and myogenin (Abcam,

Cambridge, UK) or Cx43 (Transduction Laboratories, Lexington, KY, USA) for 1 h at 37°C, then rinsed in PBS with 1% BSA and incubated with secondary antibodies conjugated with Chromeo™ 488 or Cy5 (Abcam). Analysis was performed by the Olympus imaging system composed of the Olympus IX81 microscope (Olympus Europe holding GmbH, Hamburg, Germany) with the Orca-R^2 cooled digital camera (Hamamatsu Photonics K.K., Hamamatsu City Japan), fluorescence excitation system MT10 (Olympus Life Science Europa GmbH, Hamburg, Germany) and fluorescence imaging system XCELLENCE (Olympus Soft Imaging Solutions GmbH, München, Germany).

Cell transfection with Cx43EGFP

The Cx43EGFP plasmid (Bukauskas *et al.* 2001) was transfected into cultured SMs using Lipofectamine™ 2000 and following the manufacturer's recommended protocol (Invitrogen, Carlsbad, CA, USA). Transfection efficiency was tested by Western blot (WB). The formation of Cx43EGFP GJs was visualized by the Olympus imaging system and examined by the dual whole-cell patch-clamp technique. The cells were cultured in the presence of 300–500 μg/ml geneticin to obtain a stable transfected cell line.

Immunoblot assay

Cells were lysed in ice-cold lysis buffer (50 mM Tris pH 7.5, 50 mM NaCl, 1 mM EDTA, 1 mM EGTA, 50 mM NaF, 1% Triton X-100, 1 mM β-glycerophosphate, 1 mM Na_3VO_4 and protease inhibitor cocktail 1:50). Then samples were centrifuged at 13,000 ***g*** and 4°C for 15 min, and supernatants were placed into new Eppendorf tubes. Protein concentrations were estimated by the Bradford assay (Bio-Rad, Berkeley CA, USA). Before loading onto the gel, protein samples were dissolved in loading buffer [3× SDS sample buffer: 188 mM Tris-HCl (pH 6.8), 4% SDS, 30% glycerol, 2% β-mercaptoethanol, 0.02% bromophenol blue] at a final 1× concentration and heated at 95°C for 5 min. Equal amounts of protein were separated by SDS-PAGE on 10% acrylamide gels. The proteins separated on the gel were transferred to the PVDF membrane (GE Healthcare, CA, USA) and then were blocked with blocking buffer containing 5% low-fat milk or 5% BSA in TBST (50 mM Tris pH 7.6, 150 mM NaCl, 0.05% Tween-20) for 1 h at room temperature. PVDF membranes were probed with primary antibodies against Cx43 for detection of endogenous Cx43 in case of wild-type SMs (Transduction Laboratories) and GFP for detection of only exogenous Cx43EGFP in case of Cx43EGFP-transfected SMs (Invitrogen) in TBST with 5% BSA for 24 h at 4°C and after washing with TBST solution were incubated for 1 h at room temperature with secondary antibodies – goat anti-mouse and goat anti-rabbit Fab fragment, respectively, conjugated with alkaline phosphatase (Invitrogen). Proteins were visualized by the alkaline phosphatase method (Carl Roth GmbH & Co. KG, Karlsruhe, Germany).

Induction of MI and transplantation of SMs

New Zealand white rabbits of both genders, aged 6–12 months and weighing 3.0–3.5 kg, were used in this study. The rabbits were anaesthetized with Bioketan (35 mg/kg) and Xylazine (5 mg/kg) and mechanically ventilated at 60 breathes/min through a 3.0- to 3.5-mm endotracheal tube without manchette. Glucose solution (5%) was injected intravenously during anaesthesia. The heart was exposed by a left thoracotomy incision via the 4-5 intercostal space. The left anterior descending coronary artery was ligated with a 7-0 monofilament polypropylene suture in the middle or S6–S7 segments. Before operation, the rabbits were treated with antibiotics Enroxil (5%, 0.5 ml/kg); after operation, 1 ml of Rapidexon (nonsteroidal anti-inflammatory drug) 1 time/day (3 days), 1 ml of Novasul (analgesic) 1–2 times/day (for 3 days) and Enroxil (5%, 0.1 ml/kg) 1 time/day (5 days) were administered.

One hour after induction of MI, 0.5 ml of IMDM containing approximately 6 million cells or 0.5 ml of only IMDM was injected into the MI region through a 30-gauge needle at 8–10 sites. Before transplantation, wild-type SM membranes were labelled with PKH26, a fluorescent dye, following the manufacturer's recommended protocol.

Echocardiography

Left ventricular (LV) systolic function was monitored under general anaesthesia by 7-MHz Acuson Cypress ultrasound equipment before MI, after MI and periodically within 3 months after myoblast transplantation. LVEF was calculated using the modified Simpson's rule. LV wall motion score index (WMSI) was derived as a sum of wall motion scores of 16 individual LV segments (Figure 3a) divided by the number of segments visualized (Schiller *et al.* 1989). Each segment was given a score based on its systolic function: 1, normal kinetics (grey); 2, hypokinesis (green); 3, akinesis (yellow); 4, dyskinesis (red); and 5, aneurism.

Optical mapping of cardiac electrical activity

The rabbits were anaesthetized intravenously with an injection of sodium thiopental (50 mg/kg) together with anticoagulant heparin (1000 U/kg). The hearts were quickly removed and placed into the St. Thomas solution. Then the modified Langendorff system was used to perfuse the hearts with oxygenated Solution #1 (see subchapter *Solution*s below) at 37°C at a flow rate of 17–18 ml/min. To eliminate movement artefacts contraction of the heart was arrested by adding 20 μM (±)-blebbistatin and 5 mM 2,3-butanedione monoxime (BDM). di-4-ANEPPS (20 ml, 10 μM), a potential sensitive dye, was applied to the heart by adding it to the perfusion solution. The dye was excited with 520-nm light, and emitted light was filtered at 650 nm and recorded with the cooled fast Andor iXon EMCCD camera ($iXon^{EM}$ + DU-860; Andor Technology, Belfast, UK) using the imaging software (Andor SOLIS x-3467;

Andor Technology, Belfast, UK). Optical action potential records were taken from the 5 × 5 pixel area using the ImageJ 1.45S software (public domain, NIH, Bethesda, MD, USA). For measurements of electrical activity regions of interest were selected in the healthy and infarction zones.

Enzymatic isolation of rabbit cardiac myocytes

For isolation of heart cells the rabbits were anaesthetized as described above. The atria were removed from the Langendorff-perfused heart, cut into small pieces (approximately 1 mm^3) and washed twice in Solution #2 with 30 mM BDM added to protect the tissue from hypoxic injury. Then the tissue was placed in a 25-ml flask with 10 ml of calcium-free Solution #2 containing 5 mg/ml fatty acid-free BSA, 180 U/ml collagenase (Type II; Worthington, Lakewood, NJ, USA) and 7 U/ml protease (Type XXIV) and agitated for 30 min at 37°C. Afterwards the solution was replaced by 10 ml of fresh Solution #2 containing 280 U/ml collagenase (Type II; Worthington) and BSA. After 15- to 20-min agitation, the digestive solution was replaced by a fresh one, and agitation was continued. The procedure was repeated until adequate dissociation (after 45–60 min) was achieved. All steps were carried out at 37°C with continuous gassing with 100% O_2. Then, the cell suspension was filtered through a 250-μm pore mesh, the cells were settled down and centrifuged at 500 rpm for 1 min, and the pellet was gently resuspended in enzyme and calcium-free Solution #1.

Coculturing of myoblasts and allogenic cardiac myocytes

The CMs were platted on laminin- (0.1 mg/ml) and poly-L-lysine-coated (0.1 mg/ml) glass coverslips and then placed in an incubator (37°C, 5% CO_2) for 10 h until adhesion occurred. The unattached CMs were removed, and SM suspension was applied. The plates with glass coverslips were placed in an incubator (37°C, 5% CO_2) for at least 4 h to allow SMs and CMs to form intercellular connections. IMDM containing 10% FBS, 100 U/ml penicillin, 100 μg/ml streptomycin and 10 mM BDM was used as a coculture medium.

Patch-clamp measurements

For electrophysiological recordings, glass coverslips with SMs and CMs were transferred to the experimental chamber with constant flow-through perfusion mounted on the stage of the inverted microscope Olympus IX81. Junctional conductance between the SM and the CM (abutted or connected through TTs) was measured using the dual whole-cell patch-clamp technique. Cell 1 and cell 2 of a cell pair were voltage clamped independently with the patch-clamp amplifier MultiClamp 700B (Molecular Devices, Inc., Sunyvale, CA, USA) at the same holding potential ($V_1 = V_2$). Voltages and currents were digitized using the Digidata 1440A data acquisition system (Molecular Devices, Inc.) and analysed using the pClamp 10 software (Molecular Devices, Inc.). By stepping voltage in the cell 1 (ΔV_1) and keeping the other constant, junctional current was measured as a change in current in the unstepped cell 2 ($I_j = \Delta I_2$). Thus, g_j was obtained from the ratio $-I_j/\Delta V_1$, where ΔV_1 is equal to transjunctional voltage (V_j), and a negative sign indicates that junctional current measured in the cell 2 is oppositely oriented to the one measured in the cell 1. To minimize the effect of series resistance on g_j measurements (Wilders & Jongsma 1992), we maintained pipette resistances below 3 MOhms. Patch pipettes were pulled from borosilicate glass capillary tubes with filaments. Experiments were performed at room temperature in Solution #3. Patch pipettes were filled with Solution #4.

To record $I_{Ca,L}$, the cells were depolarized every 8 s from a holding potential of −80 mV by a short prepulse (50 ms) to −50 mV and then to 0 mV for 400 ms. Prepulse and/or application of TTX were used to eliminate fast sodium currents. K^+ currents were blocked by replacing all K^+ ions with intracellular and extracellular Cs^+.

Histological analysis

Histological analysis of LV sections was performed using Axio Imager Z1 (Carl Zeiss, Oberkochen, Germany) and software AxioVision 4.7.1 (Carl Zeiss). The slices were stained with haematoxylin/eosin and were analysed under a light microscope. If the cells before transplantation were transfected with Cx43EGFP or labelled with DAPI and PKH26, fluorescence microscopy was applied.

Solutions

All reagents were purchased from Sigma-Aldrich Corp. (Steinheim, Germany) unless otherwise specified.

Solution #1 is Tyrode solution (in mM):
NaCl, 135; KCl, 5.4; $CaCl_2$, 1.8; $MgCl_2$, 0.9; NaH_2PO_4, 0.33; glucose, 10; and HEPES, 10 (pH 7.4 adjusted with NaOH).

Solution #2 is modified calcium-free Tyrode solution (in mM):
NaCl, 120; KCl, 5.8; $NaHCO_3$, 4.3; KH_2PO_4, 1.3; $MgCl_2$, 1.5; glucose, 14.1; and HEPES, 20 (pH was adjusted to 7.15 with NaOH).

Solution #3 is Krebs–Ringer solution (in mM):
NaCl, 140; KCl, 4; $CaCl_2$, 2; $MgCl_2$, 1; glucose, 5; pyruvate, 2; HEPES, 5 (pH 7.4).

Solution #4 is patch pipette solution (in mM):
KCl, 130; Na aspartate, 10; MgATP, 3; $MgCl_2$, 1; $CaCl_2$, 0.2; EGTA, 2; HEPES, 5 (pH 7.3).

Statistical analysis

The data are reported as means ± SEM. Statistical analysis was performed using the Student's *t*-test or ANOVA analysis with the *post hoc* Bonferroni test. Differences were considered statistically significant at $P < 0.05$.

Results

Characterization of rabbit skeletal muscle-derived cells

Desmin, a muscle-specific marker, was used to evaluate the purity of SM cultures prepared from the rabbit femoral muscle (Zhu *et al.* 2010). The overwhelming majority (99%) of the cells were desmin positive (Figure 1a). Myogenin, a myogenic differentiation marker, was observed in approximately 80% of the cell nuclei (Figure 1b). Figure 1(c,d) shows the expression of endogenous Cx43WT and exogenous Cx43EGFP, respectively, and the formation

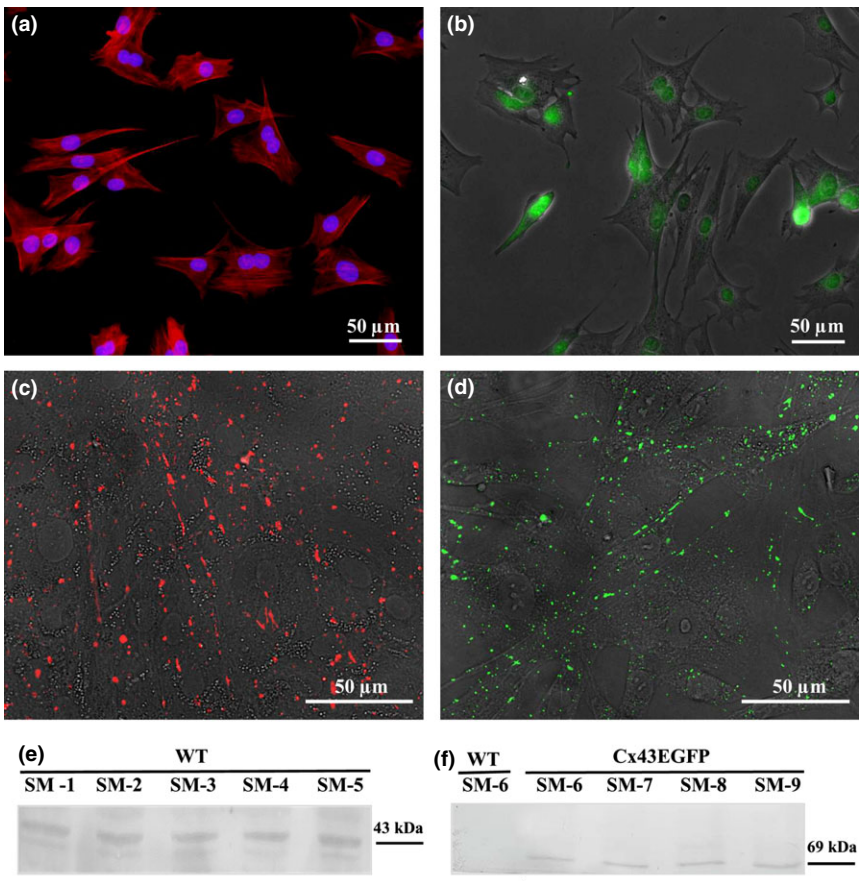

Figure 1 Characterization of skeletal myoblasts. (a) Desmin (blue nucleus labelled with DAPI), (b) myogenin, (c) endogenous Cx43WT labelled with anti-Cx43, (d) exogenous Cx43EGFP, (e) expression of endogenous Cx43 in different cell lines (CM1-CM5) and (f) expression of exogenous Cx43EGFP in different cell lines (CM6-CM9). CM, cardiomyocyte.

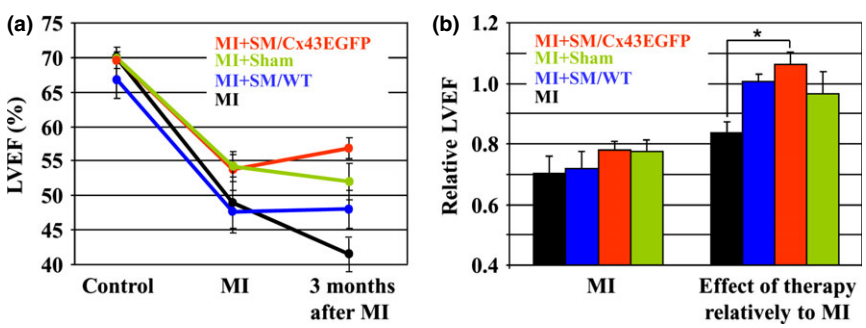

Figure 2 Dynamics of changes in LV ejection fraction. (a) Measurements of left ventricular ejection fraction (LVEF) before myocardial infarction (MI); when the myocardium has stabilized after MI, and 3 months after MI. (b) Relative LVEF in groups after MI, relatively to control (left panel; each bar is derived from the respective measurement in (a) and expressed as a ratio of LVEF values at MI and at Control); and 3 months after MI, relatively to respective MI (right panel; each bar is derived from the respective measurement in (a) and expressed as a ratio of LVEF values at 3 months after MI and at MI). $n = 5$ in each group. LV, left ventricular.

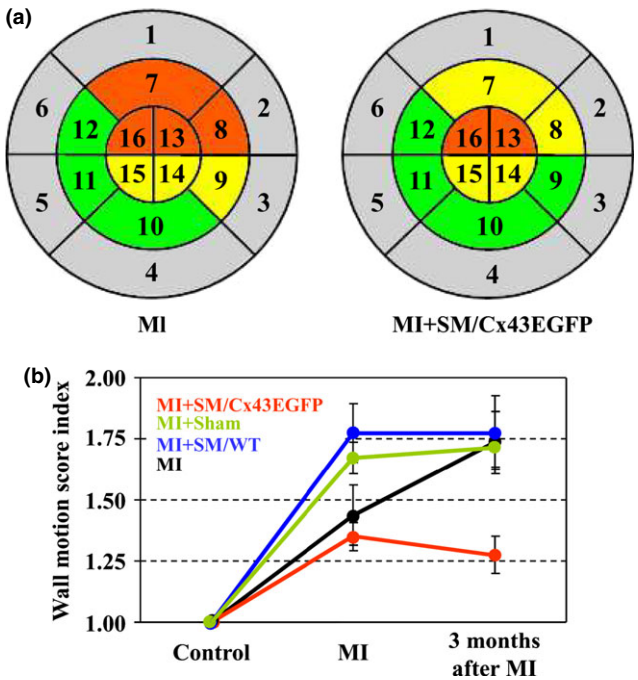

Figure 3 Evaluation of left ventricular (LV) regional function by 2D echocardiography. (a) Myocardial infarction (MI) caused a reduction of LV contractility evaluated in 16 segments (grey, normal kinetics; green, hypokinesis; yellow, akinesis; red, dyskinesis). (b) Comparison of LV WMSI dynamics between experimental groups. WMSI, wall motion score index.

of GJ plaques between SMs in the culture. The SMs expressing Cx43EGFP *in vitro* formed functional GJ plaques, visible as multiple 1- to 5-μm green dots. The mean conductance between only Cx43WT-expressing SMs and between Cx43EGFP-transfected SMs was 9 ± 1 nS (n = 15; varied from 2 to 18 nS) and 15 ± 2 nS (n = 20; varied from 2 to 29 nS; $P < 0.05$), respectively, as measured by the dual whole-cell patch-clamp technique. Also, in the selected cell lines, we verified the expression of Cx43WT and Cx43EGFP proteins by WB using anti-Cx43 and anti-GFP antibodies respectively (Figure 1e,f).

Evaluation of cardiac function and survival of engrafted cells

According to the procedures performed after MI, the animals were subdivided into four groups: (i) SM/WT (n = 5): rabbits injected with wild-type SMs (approximately 6 million cells in 0.5 ml IMDM; labelled with PKH-26); (ii) SM/Cx43EGFP (n = 5): rabbits injected with Cx43EGFP-transfected SMs (approximately 6 million cells in 0.5 ml IMDM); (iii) Sham (n = 5): rabbits injected with a cell culture medium (0.5 ml IMDM); and (iv) MI (n = 5): untreated rabbits (no cell or medium injection).

Left ventricular ejection fraction. After MI, LVEF decreased in all groups by 26 ± 4.5% ($P < 0.01$). To evaluate the effect of stem cell therapy, we measured LVEF at 3 months after MI. Dynamics of changes in LVEF is shown in Figure 2(a,b). After the acute period of MI, LVEF continued to decrease in the MI group (additional drop by 16.3 ± 3.6%; $P < 0.05$), remained stable in the Sham and SM/WT groups (96.5 ± 7.2%; and 100.7 ± 2.2%, respectively; $P > 0.05$) and increased in SM/Cx43EGFP group (106 ± 4.1%; $P > 0.05$). Figure 2(b) (right panel) shows

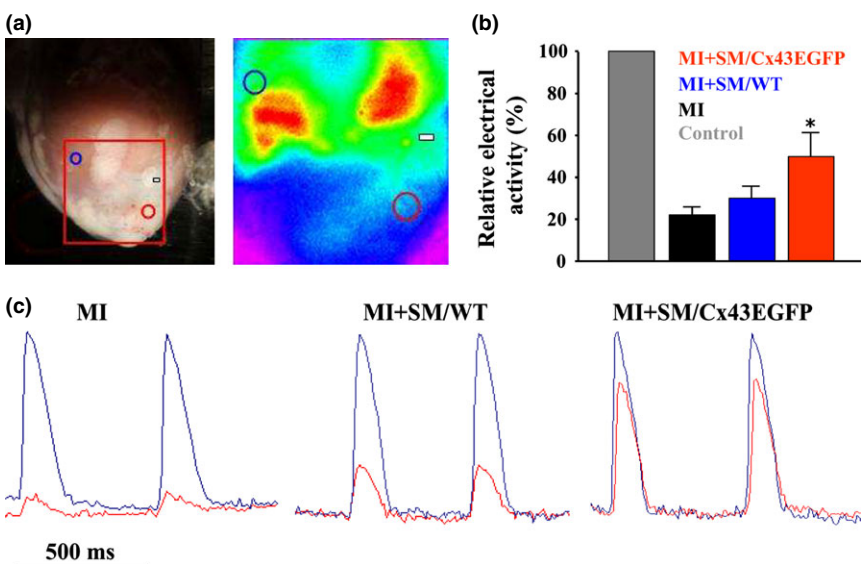

Figure 4 Electrical activity in Langendorff-perfused rabbit hearts measured by optical mapping. (a) Electrical activity was measured in the healthy myocardium (blue circle) and infarction zone (red circle). Artery ligation site is indicated by rectangular. (b) Relative values of electrical activities in the examined groups (*$P < 0.05$ between myocardial infarction (MI) and MI + SM/Cx43EGFP groups). (c) Normalized typical optical action potentials in the healthy (blue traces) and infarction (red traces) zones of MI, SM/WT and SM/Cx43EGFP groups. SM, skeletal myoblast.

that only SM/Cx43EGFP group demonstrated a significant improvement in LVEF 3 months after infarction as compared to the MI group ($P < 0.05$).

LV regional function. Dynamics of changes in the LV WMSI was evaluated by 2D echocardiography (Figure 3a, b). The WMSI dramatically increased during the acute period of MI in all groups and continued to increase in the MI group, remained stable in the Sham and SM/WT groups and slightly recovered in the SM/Cx43EGFP group at 3 months after MI ($P < 0.05$ compared to the MI group).

Electrical activity in the healthy and damaged zone of the heart was measured *ex vivo* in Langendorff-perfused hearts by optical mapping using di-4-ANEPPS, a potential sensitive fluorescent dye (Figure 4a). Electrical activity in the MI zone as compared with the healthy zone was 4.8 ± 0.1, 3.3 ± 0.1 and 2.0 ± 0.2 fold lower in the MI, SM/WT and SM/Cx43EGFP groups respectively (Figure 4a). The significant recovery of electrical activity 3 months after MI was achieved only in the SM/Cx43EGFP group compared with the MI group ($P < 0.05$). Optical recordings of typical action potentials in the healthy and infarction zones are shown in Figure 4(a).

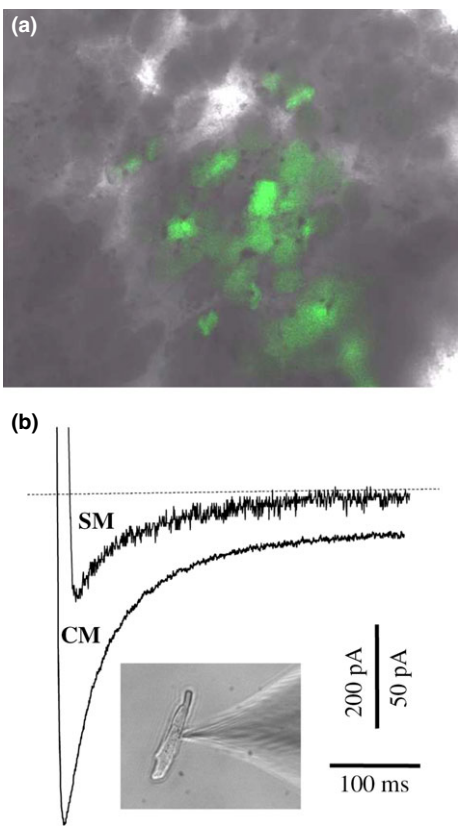

Figure 5 Comparison of $I_{Ca,L}$ amplitudes in healthy cardiomyocytes (CMs) and implanted skeletal myoblasts (SMs). (a) Cx43EGFP-transfected SM cluster identified during enzymatic isolation from the specimen of the infarction zone. (b) Typical amplitudes of the $I_{Ca,L}$ measured in the healthy CMs and SMs derived from the infarction zone.

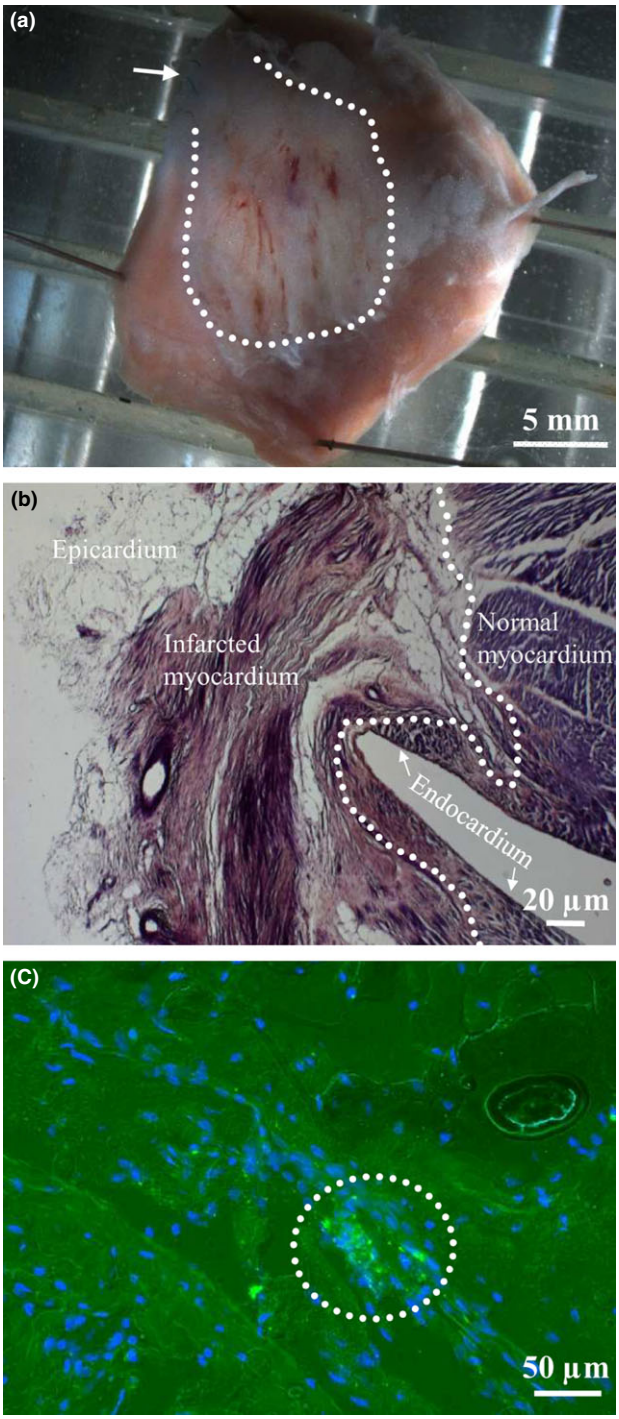

Figure 6 Anatomical and histological preparations of the left ventricle 3 months after SM implantation. (a) Epicardial view of the left ventricle with the outlined infarcted zone (arrow indicates the site of ligation of the left anterior descending coronary artery). (b) The cross-sectioned wall of the left ventricle shown in (a) stained by eosin and haematoxylin method to illustrate the healthy and infarcted myocardium. A dotted line demarcates the normal and infarcted myocardium. (c) The MI zone with accumulation of Cx43EGFP-expressing CMs (encircled). Nuclei are stained with DAPI (blue). CMs, cardiomyocytes; MI, myocardial infarction; SM, skeletal myoblast.

$I_{Ca,L}$. Having finished the optical mapping experiments, we attempted to enzymatically isolate cells from the healthy and infarction zones and to compare the amplitudes of $I_{Ca,L}$. Implanted SMs were recognized by PKH26 or EGFP fluorescence in the SM/WT or SM/Cx43EGFP groups respectively (Figure 5a). In the implanted cells, which we succeeded to isolate from the infarction zone, the amplitude of $I_{Ca,L}$ was 93 ± 15 pA (n =5), while in the healthy myocytes, it was 478 ± 62 pA (n = 8; $P < 0.001$; Figure 5b), similar to that measured in ventricular myocytes of New Zealand rabbits by other authors (Tohse *et al.* 1995; Rozanski *et al.* 1997).

Histology. Images of the cardiac tissue after MI are presented in Figure 6. Figure 6(a) shows a general epicardial view of the left ventricle after MI (an arrow indicates the site of ligation of the left anterior descending coronary artery; a dotted line denotes the infarction zone). Figure 6(b) demonstrates the cross-sectioned wall of the left ventricle shown in Figure 6(a). A uniform structure of normally organized CMs is disarranged in the infarcted zone. Figure 6(c) shows that Cx43EGFP-transfected SMs were successfully engrafted and integrated in the affected LV tissue.

Cell-to-cell coupling. Histological examination and optical mapping demonstrated that after MI, only few myocytes survived, and electrical activity was very low in the MI zone. Therefore, we raised a question how implanted SMs can establish electrical communication with host myocytes of the transitional zone under so severe conditions. Even though implanted myocytes survive, they have very low chances to form the functional homogenous electrical network with myocytes allowing the improvement of mechanical function of the heart. Moreover, the islands of implanted SMs may be arrhythmogenic. To form the homogenous electrical network, first of all, SMs must establish GJ-based electrical communication with CMs. This is impossible if the number of surrounding myocytes is insufficient. However, as we have demonstrated by measuring LVEF, a slight recovery of mechanical function was achieved following the transplantation of SMs transfected with Cx43EGFP. To verify whether SMs can form GJs with abutted CMs (Figure 7a), we cocultured these two types of cells and performed dual whole-cell patch-clamp measurements. Figure 7(e) displays the g_j/V_j plot obtained by measuring the I_j response (Figure 7d) in the SM to the voltage ramp of negative polarity from 0 to −120 mV (Figure 7c) applied to the CM. The presence of voltage gating indicates that the cells established electrical coupling by forming functional GJs. The measured g_j between four cell pairs was approximately 10 nS on average. Then, we raised a hypothesis that even in the absence of adjacent CMs, SMs may establish electrical coupling with remote CMs by growing lamellipodium- or filopodium-based extensions and forming TT-like intercellular bridges. Indeed, as shown in Figure 7(b), in coculture, we identified the CMs connected to SMs through TTs. Figure 7(g) demonstrates the g_j/V_j plot

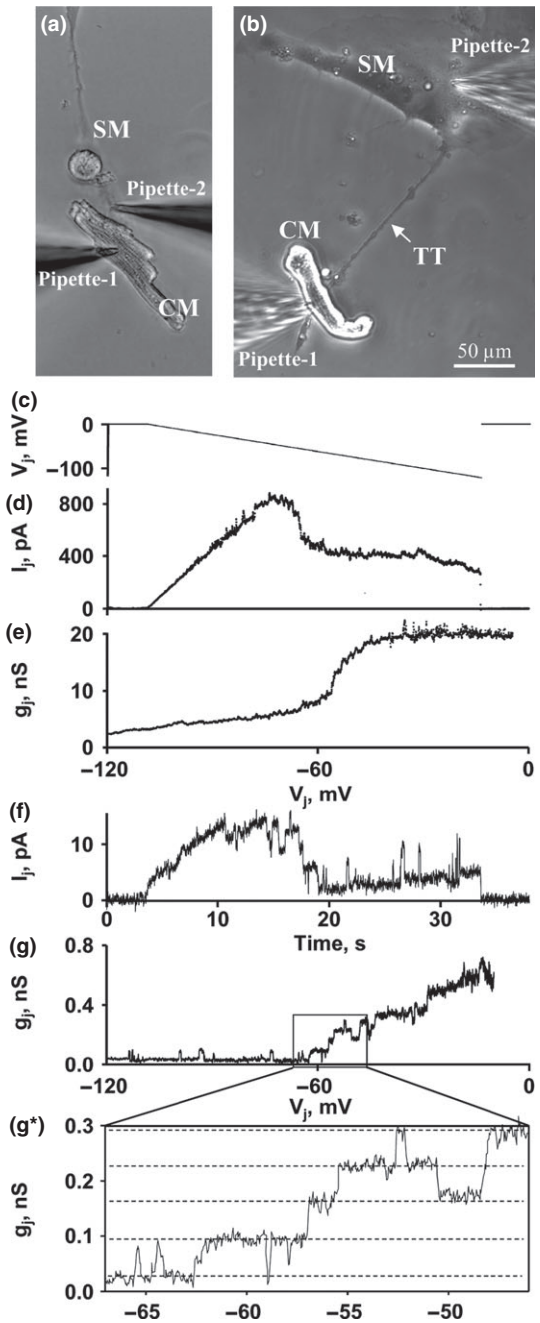

Figure 7 Electrical coupling between cardiomyocytes (CMs) and skeletal myoblasts (SMs). (a) The measurement of electrical coupling between abutted CM and SM. (b) The measurement of electrical coupling between the CM and the SM connected through the tunnelling tube (TT). (c–e) Electrical coupling between the abutted cells was measured by applying the voltage ramp of negative polarity from 0 to −120 mV to the CM and measuring I_j and g_j/V_j in the SM. g_j/V_j dependence is calculated from I_j response to V_j ramp. (f,g) Electrical coupling between the cells connected through the TT was measured by applying the voltage ramp of negative polarity from 0 to −120 mV to the CM and measuring I_j and g_j/V_j in the SM. (g*) An inset demonstrates several single channel (dotted lines) openings typical of Cx43 [gap junction (GJs)].

obtained by measuring the I_j response (Figure 7f) in the SM to the voltage ramp of negative polarity from 0 to −120 mV (Figure 7c) applied to the CM. The presence of voltage gating indicates that the cells established electrical coupling by forming functional GJs. The electrical coupling measured between four cell pairs was approximately 1 nS on average, that is about 10-fold lower than that between the abutted cells. Due to low conductance between the cells, even single channel openings could be seen (Figure 7g,g*). The measured single channel conductance was approximately 90 pS, that is typical of Cx43 channels (González *et al.* 2007).

Discussion and conclusions

Benefits of SM therapy

In the present study, we have demonstrated that the transplantation of autologous SMs expressing exogenous Cx43EGFP ameliorated the mechanical function and electrical activity of the rabbit heart after experimentally induced MI. The expression of exogenous Cx43EGFP was crucial for obtaining this positive effect because in the control series of experiments (MI group), after infarction, LVEF continued to decrease within 3 months of observation. Interestingly, we observed some stabilization of LVEF in the Sham and SM/WT groups. We suppose that this stabilization could be achieved by mobilization of endogenous stem cells to the infarction zone that was mechanically injured by transplantation procedure and/or due to paracrine secretions and scar remodelling (Catelain *et al.* 2013). Histological examination confirmed survival and incorporation of transplanted SMs in the infarction zone. Under our experimental conditions the possible development of tachyarrhythmias was prevented by continuous administration of anti-arrhythmic drugs and by induced expression of Cx43EGFP because it is known that in SMs, the endogenous Cx43 is downregulated during myogenic differentiation, and therefore, the transplantation of wild-type SMs can be hardly expected to possess therapeutic potential and can cause arrhythmias (Roell *et al.* 2007). Even Cx43EGFP-transfected SMs have a low chance of forming a functional homogenous electrical network with myocytes because only few myocytes survive after infarction, as is known from other studies (Mani & Kitsis 2003), and as follows from our measurements of electrical activity in the healthy and infarction zones. Under such conditions membranous TTs (reviewed in Abounit & Zurzolo 2012) may play an important role in establishing GJ-based electrical communication between SMs and remote CMs. To our knowledge the current study is the first showing that rabbit SMs and allogenic CMs, at least in coculture, were capable of establishing electrical communication over long distances (up to approximately 400 μm) through TTs, while other authors have demonstrated this between CMs and cardiac fibroblasts (He *et al.* 2011) as well as between CMs and endothelial progenitor cells (Koyanagi *et al.* 2005). On the other hand, the longest TTs (up to approximately 700 μm), which form between SMs during their division and subsequent dislodgment and usually do not contain GJs (not shown), may facilitate survival and proliferation of implanted cells by maintaining homeostasis and energy demands. Our recent work (Antanaviciute *et al.* 2014b) and publications by other authors (Koyanagi *et al.* 2005; Pasquier *et al.* 2013) demonstrate that TTs not only can couple cells electrically and transfer metabolites but also transport mitochondria. Moreover, TTs can transfer genetic material such as miRNA or siRNA (Antanaviciute *et al.* 2014b), which may play an important role in myogenic differentiation of SMs (Formigli *et al.* 2009).

Limitations of SM therapy

Even though SM/Cx43EGFP transplantation generated modest therapeutic effect under our experimental conditions, much better effect was achieved on electrical activity in the infarction zone as demonstrated by optical mapping using potential sensitive optical dyes. This finding suggests that a more pronounced therapeutic effect was not achieved due to insufficient excitation–contraction coupling and/or underdevelopment of the contractility apparatus during the myogenic differentiation of SMs. During cardiac action potential, L-type voltage-dependent calcium channels (L-VDCC) are activated and trigger Ca^{2+} release from the sarcoplasmic reticulum to provide Ca^{2+} for activation of myofilaments, which cause the contraction (Bers 2002). Myocytes from skeletal muscle have higher Ca^{2+} gain from the sarcoplasmic reticulum than myocytes of the cardiac muscle. In SMs, Ca^{2+} channels ($Ca_v1.1$) interact directly with the ryanodine-sensitive Ca^{2+} release channels (RyR1) of the sarcoplasmic reticulum, while in CMs, Ca^{2+} entry through Ca^{2+} channels ($Ca_v1.2$) is required to activate ryanodine receptors (RyR2) and initiate Ca^{2+}-induced Ca^{2+} release (Catterall 2011). A dramatic raise in the intracellular Ca^{2+} concentration allows Ca^{2+} to bind to myofilament protein troponin C, which initiates myocyte contraction. The mishandling of Ca^{2+} by a myocyte is a major cause of contractile dysfunction. Even though the SM/Cx43EGFP transplantation led to substantial recovery of electrical activity in the infarction zone under our experimental conditions, it was not accompanied by the recovery of contraction force. We envisage the following reasons for this discrepancy:

- It has been shown that after SM engraftment, L-VDCCs may downregulate (Ott *et al.* 2004). Our patch-clamp measurements advocate this possibility as we found that $I_{Ca,L}$, recorded in SMs isolated 3 months after transplantation, was several fold smaller than that in the healthy CMs, while in the culture both types of cells exhibited comparable $I_{Ca,L}$ amplitudes or current densities (Tohse *et al.* 1995; Rozanski *et al.* 1997; Held *et al.* 2002).
- Sarcomere underdevelopment or insufficient sensitivity of myofilaments to Ca^{2+} (Reinecke *et al.* 2002). It has been shown by other authors that SMs *in vitro* and *in vivo* may lose their myogenicity (Machida *et al.* 2004; Montarras *et al.* 2005).

Perspectives of SMs

High proliferative potential, resistance to ischaemia and myogenic differentiation of SMs make them one of the most attractive candidates among different types of stem cells for application in cellular therapy. However, experimental studies have revealed the inability of SMs to couple directly with the native myocardium and increased risk of tachyarrhythmias after implantation. These disadvantages can be overcome by the exogenous expression of Cx43 as it has been demonstrated in this study and by Roell *et al.* (2007).

We believe that better results could be achieved by reopening of the blocked artery after MI; however, we worried that this could cause the occurrence of reperfusion-induced arrhythmias and followed the acute infarction model reviewed by other authors (Kolk *et al.* 2009; Ou *et al.* 2012). Also, different results could be achieved using the chronic infarction model that is more complicated to perform but is closer to clinical practice, that is patients after MI do not undergo coronary artery bypass graft surgery immediately as some recovery period is needed during which autologous SMs can be prepared for transplantation during the same operation.

As an alternative for SM injection, muscle tissue engineering using SMs grown in three-dimensional (3D) synthetic porous scaffolds has been proposed for heart regeneration. For the creation of 3D artificial tissues with SMs, the decellularized cardiac matrix (Tapias & Ott 2014) or synthetic biomaterials mimicking the properties of the heart matrix can be used. Also, cells can be cultured in a hydrogel and induced to produce and assemble their own matrix (Vunjak-Novakovic *et al.* 2010). Bioreactors can be used to deliver cytokines and other bioactive molecules for the control of SM differentiation (Liu *et al.* 2013). Finally, electrical and mechanical stimulation has been shown to be essential for the formation of contracting tissue (Serena *et al.* 2008) and increase of cell proliferation (Pedrotty *et al.* 2005).

Thus, future challenges in the engineering of SM-based artificial cardiac patches or injectable scaffolds will involve the right selection and combination of biomaterials; optimal concentration of exogenous Cx43-expressing SMs; size of the scaffold; composition of culture medium aimed at developing desirable properties of SMs; parameters of electrical and/or mechanical stimulation; and methods of engraftment ensuring electrical and metabolic integration and vascularization of the tissue.

Funding source

This work was supported by a grant (No. LIG-13/2012) from the Research Council of Lithuania and by a grant (No. B-26/2007) from Lithuanian State Science and Studies Foundation.

Conflict of interest

The authors declare that they have no competing interests.

References

Abounit S. & Zurzolo C. (2012) Wiring through tunneling nanotubes–from electrical signals to organelle transfer. *J. Cell Sci.* **125**, 1089–1098.

Abraham M.R., Henrikson C.A., Tung L. *et al.* (2005) Antiarrhythmic engineering of skeletal myoblasts for cardiac transplantation. *Circ. Res.* **97**, 159–167.

Antanaviciute I., Mildaziene V., Stankevicius E., Herdegen T. & Skeberdis V.A. (2014a) Hyperthermia differently affects connexin43 expression and gap junction permeability in skeletal myoblasts and HeLa cells. *Mediators Inflamm.* **2014**, 748290.

Antanaviciute I., Rysevaite K., Liutkevicius V. *et al.* (2014b) Long-distance communication between laryngeal carcinoma cells. *PLoS ONE* **9**, e99196.

Balogh S., Naus C.C. & Merrifield P.A. (1993) Expression of gap junctions in cultured rat L6 cells during myogenesis. *Dev. Biol.* **155**, 351–360.

Bers D.M. (2002) Cardiac excitation-contraction coupling. *Nature* **415**, 198–205.

Brickwedel J., Gulbins H. & Reichenspurner H. (2014) Long-term follow-up after autologous skeletal myoblast transplantation in ischaemic heart disease. *Interact. Cardiovasc. Thorac. Surg.* **18**, 61–66.

Bukauskas F.F., Bukauskiene A., Bennett M.V. & Verselis V.K. (2001) Gating properties of gap junction channels assembled from connexin43 and connexin43 fused with green fluorescent protein. *Biophys. J.* **81**, 137–152.

Catelain C., Riveron S., Papadopoulos A. *et al.* (2013) Myoblasts and embryonic stem cells differentially engraft in a mouse model of genetic dilated cardiomyopathy. *Mol. Ther.* **21**, 1064–1075.

Catterall W.A. (2011) Voltage-gated calcium channels. *Cold Spring Harb. Perspect. Biol.* **3**, a003947.

Durrani S., Konoplyannikov M., Ashraf M. & Haider K.H. (2010) Skeletal myoblasts for cardiac repair. *Regen. Med.* **5**, 919–932.

Fernandes S., Amirault J.C., Lande G. *et al.* (2006) Autologous myoblast transplantation after myocardial infarction increases the inducibility of ventricular arrhythmias. *Cardiovasc. Res.* **69**, 348–358.

Fernandes S., van Rijen H.V., Forest V. *et al.* (2009) Cardiac cell therapy: overexpression of connexin43 in skeletal myoblasts and prevention of ventricular arrhythmias. *J. Cell Mol. Med.* **13**, 3703–3712.

Formigli L., Francini F., Nistri S. *et al.* (2009) Skeletal myoblasts overexpressing relaxin improve differentiation and communication of primary murine cardiomyocyte cell cultures. *J. Mol. Cell. Cardiol.* **47**, 335–345.

González D., Gómez-Hernández J.M. & Barrio L.C. (2007) Molecular basis of voltage dependence of connexin channels: an integrative appraisal. *Prog. Biophys. Mol. Biol.* **94**, 66–106.

Haider H. & Ashraf M. (2009) Preconditioning and stem cell survival. *J. Cardiovasc. Transl. Res.* **3**, 89–102.

Haider H., Ye L., Jiang S. *et al.* (2004) Angiomyogenesis for cardiac repair using human myoblasts as carriers of human vascular endothelial growth factor. *J. Mol. Med.* **82**, 539–549.

Haider H., Jiang S., Idris N.M. & Ashraf M. (2008) IGF-1-overexpressing mesenchymal stem cells accelerate bone marrow stem cell mobilization via paracrine activation of SDF-1alpha/CXCR4 signaling to promote myocardial repair. *Circ. Res.* **103**, 1300–1308.

Hassan N., Tchao J. & Tobita K. (2014) Concise review: skeletal muscle stem cells and cardiac lineage: potential for heart repair. *Stem Cells Transl. Med.* **3**, 183–193.

He K., Shi X., Zhang X. *et al.* (2011) Long-distance intercellular connectivity between cardiomyocytes and cardiofibroblasts mediated by membrane nanotubes. *Cardiovasc. Res.* **92**, 39–47.

Held B., Freise D., Freichel M., Hoth M. & Flockerzi V. (2002) Skeletal muscle L-type Ca(2+) current modulation in gamma1-deficient and wildtype murine myotubes by the gamma1 subunit and cAMP. *J. Physiol.* **539**, 459–468.

Henning R.J. (2011) Stem cells in cardiac repair. *Future Cardiol.* **7**, 99–117.

Kanemitsu N., Tambara K., Premaratne G.U. *et al.* (2006) Insulin-like growth factor-1 enhances the efficacy of myoblast transplantation with its multiple functions in the chronic myocardial infarction rat model. *J. Heart Lung Transplant.* **25**, 1253–1262.

Kofidis T., de Bruin J.L., Yamane T. *et al.* (2004) Insulin-like growth factor promotes engraftment, differentiation, and functional improvement after transfer of embryonic stem cells for myocardial restoration. *Stem Cells* **22**, 1239–1245.

Kojima A., Goto K., Morioka S. *et al.* (2007) Heat stress facilitates the regeneration of injured skeletal muscle in rats. *J. Orthop. Sci.* **12**, 74–82.

Kolanowski T.J., Rozwadowska N., Malcher A. *et al.* (2014) In vitro and in vivo characteristics of connexin 43-modified human skeletal myoblasts as candidates for prospective stem cell therapy for the failing heart. *Int. J. Cardiol.* **173**, 55–64.

Kolk M.V., Meyberg D., Deuse T. *et al.* (2009) LAD-ligation: a murine model of myocardial infarction. *J. Vis. Exp.* **32**, e1438.

Koyanagi M., Brandes R.P., Haendeler J., Zeiher A.M. & Dimmeler S. (2005) Cell-to-cell connection of endothelial progenitor cells with cardiac myocytes by nanotubes: a novel mechanism for cell fate changes? *Circ. Res.* **96**, 1039–1041.

Leobon B., Garcin I., Menasche P., Vilquin J.T., Audinat E. & Charpak S. (2003) Myoblasts transplanted into rat infarcted myocardium are functionally isolated from their host. *Proc. Natl Acad. Sci. USA* **100**, 7808–7811.

Liu M., Liu N., Zang R., Li Y. & Yang S.T. (2013) Engineering stem cell niches in bioreactors. *World J. Stem Cells* **5**, 124–135.

Machida S., Spangenburg E.E. & Booth F.W. (2004) Primary rat muscle progenitor cells have decreased proliferation and myotube formation during passages. *Cell Prolif.* **37**, 267–277.

Mangi A.A., Noiseux N., Kong D. *et al.* (2003) Mesenchymal stem cells modified with Akt prevent remodeling and restore performance of infarcted hearts. *Nat. Med.* **9**, 1195–1201.

Mani K. & Kitsis R.N. (2003) Myocyte apoptosis: programming ventricular remodeling. *J. Am. Coll. Cardiol.* **41**, 761–764.

Menasche P. (2009) Stem cell therapy for heart failure: are arrhythmias a real safety concern? *Circulation* **119**, 2735–2740.

Menasche P., Alfieri O., Janssens S. *et al.* (2008) The Myoblast Autologous Grafting in Ischemic Cardiomyopathy (MAGIC) trial: first randomized placebo-controlled study of myoblast transplantation. *Circulation* **117**, 1189–1200.

Montarras D., Morgan J., Collins C. *et al.* (2005) Direct isolation of satellite cells for skeletal muscle regeneration. *Science* **309**, 2064–2067.

Murry C.E., Wiseman R.W., Schwartz S.M. & Hauschka S.D. (1996) Skeletal myoblast transplantation for repair of myocardial necrosis. *J. Clin. Invest.* **98**, 2512–2523.

Nakamura Y., Yasuda T., Weisel R.D. & Li R.K. (2006) Enhanced cell transplantation: preventing apoptosis increases cell survival and ventricular function. *Am. J. Physiol. Heart Circ. Physiol.* **291**, H939–H947.

Ott H.C., Berjukow S., Marksteiner R. *et al.* (2004) On the fate of skeletal myoblasts in a cardiac environment: down-regulation of voltage-gated ion channels. *J. Physiol.* **558**, 793–805.

Ou L., Li W., Liu Y. *et al.* (2012) Animal models of cardiac disease and stem cell therapy. *Open Cardiovasc. Med. J.* **4**, 231–239.

Pasquier J., Guerrouahen B.S., Al Thawadi H. *et al.* (2013) Preferential transfer of mitochondria from endothelial to cancer cells through tunneling nanotubes modulates chemoresistance. *J. Transl. Med.* **11**, 94.

Pedrotty D.M., Koh J., Davis B.H., Taylor D.A., Wolf P. & Niklason L.E. (2005) Engineering skeletal myoblasts: roles of three-dimensional culture and electrical stimulation. *Am. J. Physiol. Heart Circ. Physiol.* **288**, H1620–H1626.

Reinecke H., MacDonald G.H., Hauschka S.D. & Murry C.E. (2000) Electromechanical coupling between skeletal and cardiac muscle. Implications for infarct repair. *J. Cell Biol.* **149**, 731–740.

Reinecke H., Poppa V. & Murry C.E. (2002) Skeletal muscle stem cells do not transdifferentiate into cardiomyocytes after cardiac grafting. *J. Mol. Cell. Cardiol.* **34**, 241–249.

Roell W., Lewalter T., Sasse P. *et al.* (2007) Engraftment of connexin 43-expressing cells prevents post-infarct arrhythmia. *Nature* **450**, 819–824.

Rozanski G.J., Xu Z., Whitney R.T., Murakami H. & Zucker I.H. (1997) Electrophysiology of rabbit ventricular myocytes following sustained rapid ventricular pacing. *J. Mol. Cell. Cardiol.* **29**, 721–732.

Schiller N.B., Shah P.M., Crawford M. *et al.* (1989) Recommendations for quantitation of the left ventricle by two-dimensional echocardiography. American Society of Echocardiography Committee on Standards, Subcommittee on Quantitation of Two-Dimensional Echocardiograms. *J. Am. Soc. Echocardiogr.* **2**, 358–367.

Seidel M., Borczynska A., Rozwadowska N. & Kurpisz M. (2009) Cell-based therapy for heart failure: skeletal myoblasts. *Cell Transplant.* **18**, 695–707.

Serena E., Flaibani M., Carnio S. *et al.* (2008) Electrophysiologic stimulation improves myogenic potential of muscle precursor cells grown in a 3D collagen scaffold. *Neurol. Res.* **30**, 207–214.

Shah V.K. & Shalia K.K. (2011) Stem cell therapy in acute myocardial infarction: a pot of gold or Pandora's box. *Stem Cells Int.* **2011**, 536758.

Sherman W., He K.L., Yi G.H. *et al.* (2009) Myoblast transfer in ischemic heart failure: effects on rhythm stability. *Cell Transplant.* **18**, 333–341.

Suzuki K., Smolenski R.T., Jayakumar J., Murtuza B., Brand N.J., Yacoub M.H. (2000) Heat shock treatment enhances graft cell survival in skeletal myoblast transplantation to the heart. *Circulation* **102**, III216–III221.

Tapias L.F. & Ott H.C. (2014) Decellularized scaffolds as a platform for bioengineered organs. *Curr. Opin. Organ Transplant.* **19**, 145–152.

Tohse N., Nakaya H., Takeda Y. & Kanno M. (1995) Cyclic GMP-mediated inhibition of L-type Ca2+ channel activity by human natriuretic peptide in rabbit heart cells. *Br. J. Pharmacol.* **114**, 1076–1082.

Vunjak-Novakovic G., Tandon N., Godier A. *et al.* (2010) Challenges in cardiac tissue engineering. *Tissue Eng. Part B Rev.* **16**, 169–187.

Wilders R. & Jongsma H.J. (1992) Limitations of the dual voltage clamp method in assaying conductance and kinetics of gap junction channels. *Biophys. J.* **63**, 942–953.

Yang S., Laumonier T. & Menetrey J. (2007) Heat shock pretreatment enhances porcine myoblasts survival after autotransplantation in intact skeletal muscle. *Sci. China C Life Sci.* **50**, 438–446.

Zhu W., Wang Y., Qiu G. & Chen B. (2010) Characterization of the purification and primary culture of adult canine myoblasts in vitro. *Mol. Med. Rep.* **3**, 463–468.